

DETERMINATION OF AGE AND MASS  
OF HERBIG AE/BE STARS

by

Nirbhik Chitrakar

A senior thesis submitted to the faculty of

Ithaca College

in partial fulfillment of the requirements for the degree of

Bachelor of Science

Department of Physics

Ithaca College

April 2008

Copyright © 2008 Nirbhik Chitrakar

All Rights Reserved

ITHACA COLLEGE

DEPARTMENT APPROVAL

of a senior thesis submitted by

Nirbhik Chitrakar

This thesis has been reviewed by the research advisor, senior thesis instructor,  
and department chair and has been found to be satisfactory.

---

Date

---

Luke Keller, Advisor

---

Date

---

Luke Keller, Senior Thesis Instructor

---

Date

---

Bruce Thompson, Chair

## ABSTRACT

### DETERMINATION OF AGE AND MASS OF HERBIG AE/BE STARS

Nirbhik Chitrakar

Department of Physics

Bachelor of Science

We determine the ages and mass of 20 Herbig Ae/Be (HAeBe) stars from the list in Malfait et al. (1998). We plotted our program stars on an H-R diagram and compared them with three of the most-cited pre-main sequence (PMS) evolution models for intermediate mass stars to check for consistency. We found masses of our program stars to be consistent, but the ages seem to vary by a factor of 2 to 3. We can only conclude that this discrepancy is due to the physics and the conditions used in these models. We compare these differences and attempt to explain the discrepancy.

## ACKNOWLEDGMENTS

- Thanks to Dr. Luke Keller and Department of Physics, Ithaca College for giving me the opportunity to do research in this field.
- Thanks to F. Palla and S. W. Stahler, P.A. Bernasconi, and Siess et al. for supplying the evolutionary tracks used for this thesis.



# Contents

<b>Table of Contents</b>	<b>vii</b>
<b>1 Introduction</b>	<b>1</b>
1.1 Herbig Ae/Be stars . . . . .	1
1.2 Age and Mass of Herbig Ae/Be Stars . . . . .	2
1.3 Pre-Main-Sequence Evolution . . . . .	2
<b>2 Evolutionary Models</b>	<b>5</b>
2.1 Palla & Stahler Model . . . . .	6
2.2 Bernasconi Model . . . . .	8
2.3 Siess et al. Model . . . . .	9
<b>3 Methods</b>	<b>11</b>
3.1 Stellar Luminosity and Temperature . . . . .	11
3.2 Error Analysis . . . . .	13
3.3 Mass & Age . . . . .	13
<b>4 Results &amp; Discussion</b>	<b>15</b>
<b>5 Conclusion</b>	<b>19</b>
<b>Bibliography</b>	<b>21</b>



# Chapter 1

## Introduction

### 1.1 Herbig Ae/Be stars

Herbig Ae/Be stars were first categorized by George Herbig in 1960 (Herbig 1960). They are intermediate-mass ( $M \sim 2-10 M_{\odot}$ ) pre-main-sequence stars of spectral type A, B and early F. They are the higher mass counterparts of the T Tauri stars and similarly have the Balmer series emission lines in their stellar spectra. They can have strong infrared radiation excess due to the accretion and a warm circumstellar dust. The HAeBe stars are relatively young stars ( $< 10 \text{ Myrs}$ ) still in gravitational contraction and accretion stage, and should be located to the right of the main sequence in an HR diagram. These stars are predicted to form and evolve quicker than their lower mass counterparts (T Tauri), however, not as quickly as the higher-mass stars, which reach main-sequence completely enveloped by their circumstellar dust. This allows us to directly observe the photosphere and the circumstellar disk with relatively unobscured view, enabling a detailed study of the star formation and the circumstellar disk.

## 1.2 Age and Mass of Herbig Ae/Be Stars

The stellar parameters such as age and mass are fundamental attributes of a star. For a given composition, the star's mass determines its internal structure and manner of evolution, whereas age determines where in the evolutionary sequence it is located. These parameters are used in determination of various other parameters such as radius of a star, stellar life-time, and angular momenta for disk models and orbital calculations. Thus accuracy in determination of age and mass is important to accurately determine these characteristics. A few have attempted to determine stellar age and mass for the HAeBe stars. M.E. van der Ancker et al. (1998) determined various astrophysical parameters including age and mass for 44 HAeBe stars, which were done using evolutionary tracks from Palla & Stahler (1993). Additionally, Jesús Hernández et al. (2004) used PMS evolutionary models from Bernasconi (1996) and Siess et al. (2000) to find ages and masses of 75 HAeBe stars. However, these computations are not very consistent with each other. We noticed discrepancies of about a factor of 2 to 3 in ages amongst these studies done using different models. In this thesis, we plot 20 HAeBe stars onto a Hertzsprung-Russell(HR) diagram along with these three highly cited models and their isochrones (lines of constant age) to analyze the consistency in their ages and masses.

## 1.3 Pre-Main-Sequence Evolution

Though the process of formation of a star is far from completely understood, considerable work has been done in this subject. Many have attempted to develop theoretical models to describe this process. Amongst these, the most generally accepted picture of the phenomenon is the one developed by Shu et al. (1987). The process is divided into five distinct phases.

The first phase is marked by the formation of dense molecular core inside a giant molecular cloud (GMC). These cores may initially be supported against gravitational contraction by magnetic fields and turbulence. Since the cores are more dense than their surroundings, the core accretes stuff from the cloud around it. This contraction releases gravitational potential energy as thermal energy, which is initially radiated away as the cloud is still considerably transparent. The core gradually increase in mass and it becomes increasingly unstable and eventually collapses marking the beginning of the second phase.

The collapse increases the density of the cloud making it increasingly opaque and trapping the radiation. This allows the temperature and the pressure inside the star to increase greatly halting the collapse. At around 2000K, the molecular hydrogen disintegrates into atomic hydrogen. This provides an energy sink and triggers another collapse until hydrogen ionizes. The pressure buildup from this ionization balances the infalling pressure and halts the collapse. Throughout these processes the temperature and pressure of the star increases gradually until the halt of the collapse. This point is called the Hayashi-limit. The star is in a hydrostatic equilibrium supported by the ionization pressure of hydrogen and nuclear burning of deuterium and lithium. The flow of energy from the stellar interior to the exterior is mostly convective as the internal core is not hot enough to radiate enough energy out. This causes the luminosity of the star to decrease. As the temperature gradually rises in the core, radiation slowly takes over and the luminosity of the star increases again.

All big structure like the GMC initially has some angular momentum. During the collapse, due to conservation of angular momentum, the stellar core starts to rotating faster forming a central protostar surrounded by a disk. In the third phase, a solar wind is formed along the axis of rotation of the star due to the increasing accretion of matter through the disk. This leads to dispersion of the surrounding gas and dust

terminating the infall of matter in the fourth phase. Eventually, in the fifth phase, the dust and gas in the circumstellar disk is dispersed or incorporated into a planetary system. At this point the star has joined the main-sequence, where it will stay in equilibrium sustained by hydrogen fusion until the hydrogen is depleted in its cores.

# Chapter 2

## Evolutionary Models

Evolution of a star can be analyzed using various stellar parameters. One of the most useful is a plot of luminosity vs. temperature, or a Hertzsprung-Russell(HR) diagram. Luminosity and temperature of a star can be precisely calculated from brightness of the star(magnitude) and the wavelength where the black-body radiation from the star peaks respectively. The method is explained in section 3.1. This, then, allows us to determine various properties of a star including age and mass. As a star evolves, it traces out a path on the HR diagram, as shown in figure 2. This is called an evolutionary track. Quite a few theoretical models of the evolution have been developed. The evolutionary track in the figure 2 are three of the most-cited theoretical models. These models are computed using various computational methods, with considerations of various physical phenomenons such as accretion, rotation and molecular interactions etc. Due to complications of these computational algorithms, a grand complete model of the stellar evolution has not been yet developed making it important to compare the various parameters determined by these models.

The three models we used are: Palla & Stahler (1993), Bernasconi (1996) and Siess et al. (2000). These models are evolutionary tracks on HR diagrams, as shown

in figure 1. We plotted our program stars over the models along with their isochrones and determined age and mass of our stars. This is discussed more in detail in Section 3. We found the masses to be consistent whereas ages seem to vary by a factor of 2 to 3. We realized that this might have been due to the fact that the models have different initial conditions and physics that has been taken into account. In this chapter we briefly describe each models.

## 2.1 Palla & Stahler Model

The evolutionary tracks were retrieved from Palla & Stahler (1993). This model implements a spherically symmetric accretion flow, with an initial constant mass accretion rate of  $10^{-5}M_{\odot}yr^{-1}$ . Unlike the previous standard models, the initial conditions of the stars were not arbitrarily chosen, but rather calculated using initial phases, before the Hayashi-limit, of protostellar theory, discussed in section 1.3. This is the first model to unify the effects of accretion, thermal relaxation and deuterium burning on stellar evolution.

Thermal relaxation or cooling of a star causes inhomogeneity in radiative transfer of energy from the star into space. Due to this, the star goes through nonhomogeneous contraction in the early convective stages. The star then eventually joins the classical track, i.e. of homogeneous contraction, as the radiative luminosity everywhere in the star increases and overshadows the effects of thermal cooling. This process lengthens the lifetime of the star in its initial stages.

A protostar is fully convective initially due to the steady state deuterium burning at its core. However, as this deuterium is replenished from the surrounding cloud, the temperature of the core increases and it starts to produce luminosity creating a kind of radiative-barrier against the inflow of matter from the exterior. This halts

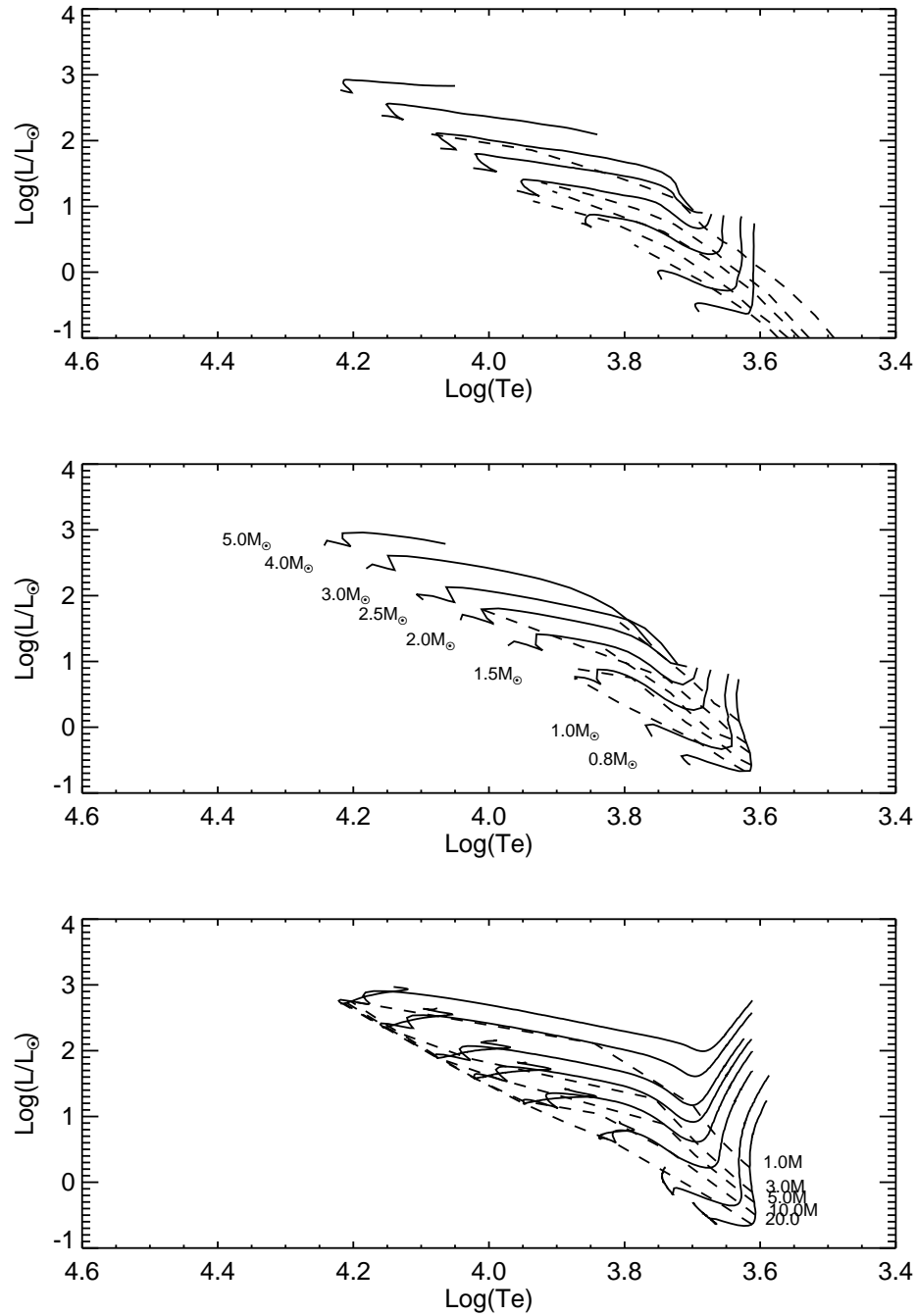


Figure 2.1 Evolutionary Tracks. Top to bottom these models were retrieved from Palla & Stahler (1993), Bernasconi (1996) and Siess et al.(2000) respectively. The solid lines are evolutionary tracks. All three models contain tracks of same masses. The corresponding masses are printed next to the tracks on the middle plot. The dotted lines are isochrones from left to right - 1.0, 3.0, 5.0, 10.0 and 20.0 million years.

the contraction of the star for sometime until the deuterium in the core is depleted. This process repeats until the deuterium burning starts taking place in the subsurface regions. This fluctuation causes a periodic contraction and expansion of the star before the temperature is hot enough for hydrogen burning. Details of these theoretical developments are described in Palla & Stahler (1994).

## 2.2 Bernasconi Model

The evolutionary tracks were retrieved from Bernasconi(1996). This model incorporates the accretion paradigm for star formation as developed by Stahler(1983) and analogs the results of Palla & Stahler(1991,1993). The birthline was improved with detailed consideration of time-dependent accretion rate, interstellar deuterium mass fraction (the amount of deuterium in the GMC), and stellar opacity (opaqueness of the cloud, related to density) as developed by Bernasconi & Maeder(1996). The effects of the first consideration only affected the birthline by around 2%. This is due to the fact that the rate of infalling material in the beginning does not vary a lot as there is very less resistance due to cold temperatures at the core. However, the consideration of deuterium mass fraction in the initial GMC increase the rate of deuterium burning, which raised the luminosity at birthline by about 10%. Additionally, they account for anisotropic time-dependent diffusion rates of deuterium in the convective shells surrounding the core. This treatment did not affect the overall nature of stellar evolution, however, this did affect time the star spent in deuterium burning equilibrium. This effect is visible in the difference in the nature of the isochrones when compared to the isochrones of Palla & Stahler model. They also accounted for relative metal(in astrophysics, metal means anything heavier than helium-4) abundances in the ISM's using Iglesias et al. (1992). This model constitutes a coherent

extension to the post-MS stellar evolution developed by the Geneva Group (Schaller et al. 1992). This provides a slightly more complete picture of the stellar evolution. Detailed theoretical formulations are described in Bernasconi & Maeder (1996).

## 2.3 Siess et al. Model

The evolutionary tracks were retrieved from Siess et al (2000). This model differs in its approach of the PMS evolution compared to the two previous models. This model is based on the Grenoble stellar evolution code described in Mowlavi & Forestini (1993). The code focuses mainly on the internal structure and microphysics inside the protostar. The atmosphere of the star is integrated with the interior by modifying pressure and temperature gradients in the stellar structure equations to account for low stellar opacity of the exterior regions. Henyey prescription is used for the internal stellar structure, along with lagrangian difference scheme based on three adjacent numerical shells. Henyey prescription refers to the original method of automatic solution of equations of stellar evolution developed and described in Henyey et al. (1955). The lagrangian difference scheme is a method of evolving the shells in the start such that their entropy is maximized. Additionally, Siess et al. in this model uses a modified equation of state to accounts the effects associated with the pressure ionization, the degeneracy conditions of stellar interior and electromagnetic interactions. This model, however, does not account effects of rotation or accretion. Schwarzschild criterion for convection is used to delimit the convective boundaries. This is a criterion where a stellar medium is stable against convection where,

$$\frac{-dT}{dZ} < \frac{g}{C_p} \quad (2.1)$$

where,  $C_p$  = heat capacity.

Additionally, instantaneous mixing inside each convective zone is assumed at each iteration during the contraction process unlike the anisotropic time-dependent diffusion rate in the Bernasconi model.

# Chapter 3

## Methods

### 3.1 Stellar Luminosity and Temperature

Most of the luminosities and effective temperatures for our program stars were obtained from various papers referenced. However, some of them had to be computed as they were not available. For  $T_{eff}$ , we matched the spectral types of the stars retrieved from SIMBAD Online Astronomical Database with the Kenyon & Hartman(1995). For luminosity, we used following formulae:

Luminosity of a star is the amount of energy radiated into space per second by a star. The log of luminosity of the star is given by,

$$\log(L_*) = -(M_{bol} - 4.74)/(2.5) \quad (3.1)$$

Bolometric magnitude,  $M_{bol}$  is the measured total of all radiation at all wavelengths from a star (bolometric means in all wavelengths). This can be computed by,

$$M_{bol} = M_V + BC \quad (3.2)$$

Magnitude of a star is the measure of the brightness of a star. There are two types of magnitudes - apparent( $m_V$ ) and absolute ( $M_V$ ). Apparent magnitude is

the magnitude as seen by an observer on earth, where as absolute magnitude is the magnitude of the star as seen by observer 10 parsecs away. These are related by the following relation,

$$M_V = m_V + 5 + 5 * \log(\pi) - A_V \quad (3.3)$$

where,

$\pi$  = stellar parallax. The angle subtended by the mean radius of Earth's orbit around the Sun as seen from the star in interest.

$A_V$  = Extinction value. The value used to describe absorption and scattering of light by dust and gas.

BC = Bolometric correction. The correction that must be made to  $M_V$  to convert from visible magnitude to  $M_{bol}$ .

Here,  $m_V$ , and BC were obtained from KH95 color table,  $\pi$  was calculated by inverting distance in parsecs.  $A_V$  was calculated as following:

color excess

$$E_{B-V} = B - V - [B - V]_0 \quad (3.4)$$

$$A_V = R * E_{B-V} \quad (3.5)$$

where,

B,V = apparent magnitudes in UBV system

$[B-V]_0$  = intrinsic color index. The expression that determines the color of a star. It gives the temperature of the star.

R = Ratio of extinction at V,  $A_V$ , to

$E_{B-V} = 2.75$  (Malfait et al, 1998)

## 3.2 Error Analysis

Error analysis was done by simply propagating the errors through the calculation. We estimated the errors in magnitude to be 1 value of the lowest significant figure. The errors in distances were obtained from their sources. Following formulae was used for propagation:

$$\delta \log(L_{\odot}) = \frac{\delta M_{bol}}{2.5} \quad (3.6)$$

$$\delta M_{bol} = \delta M_V = \sqrt{\delta m_V^2 + \delta A_v^2} \quad (3.7)$$

$$\delta A_V = R \cdot \delta E_{B-V} \quad (3.8)$$

$$\delta E_{B-V} = \sqrt{\delta B^2 + \delta V^2} \quad (3.9)$$

## 3.3 Mass & Age

Age and mass of these stars were calculated using the canonical approach, i.e. to plot the stars onto a HR diagram over the evolutionary tracks and their isochrones and find the corresponding mass and age for the position of the star in the diagram. The results are shown in figure 2. The actual values are shown in table 1.



# Chapter 4

## Results & Discussion

From the results displayed in figure 2 and table 1, we can see the masses computed from all the models were found to be fairly consistent with standard deviation of  $\#$ . However, there seems to be a discrepancy in ages by a factor of 2 to 3. After examinations of details of the models, it was clear that this is due difference in physical characteristics of the models. In section 2.2, we discussed the difference in the nature of the isochrones due to the anisotropic time-dependent diffusion rate. It is thus expected that ages computed from different models to vary.

Additionally, we noticed that few of our program stars lie below the ZAMS in all three models. Hernández et al. (2004) attempted to re-calculate the spectral types of all 77 HAeBe stars. They argued the use of higher total-to-selective extinction ratio,  $R_v$ , of around 5 compared to the standard 3.1. This did make the stars appear to be a bit younger and resolved the problem to some extent, however, few stars still exist below the ZAMS.

Another possibility we considered is the accretion rate of the stars. We noticed that Palla & Stahler model used a constant accretion rate of  $10^{-5}M_{\odot}yr^{-1}$ . In contrast, James Muzerolle et al. (2004) calculated Ae star UX Ori to be around  $10^{-8}M_{\odot}yr^{-1}$ .

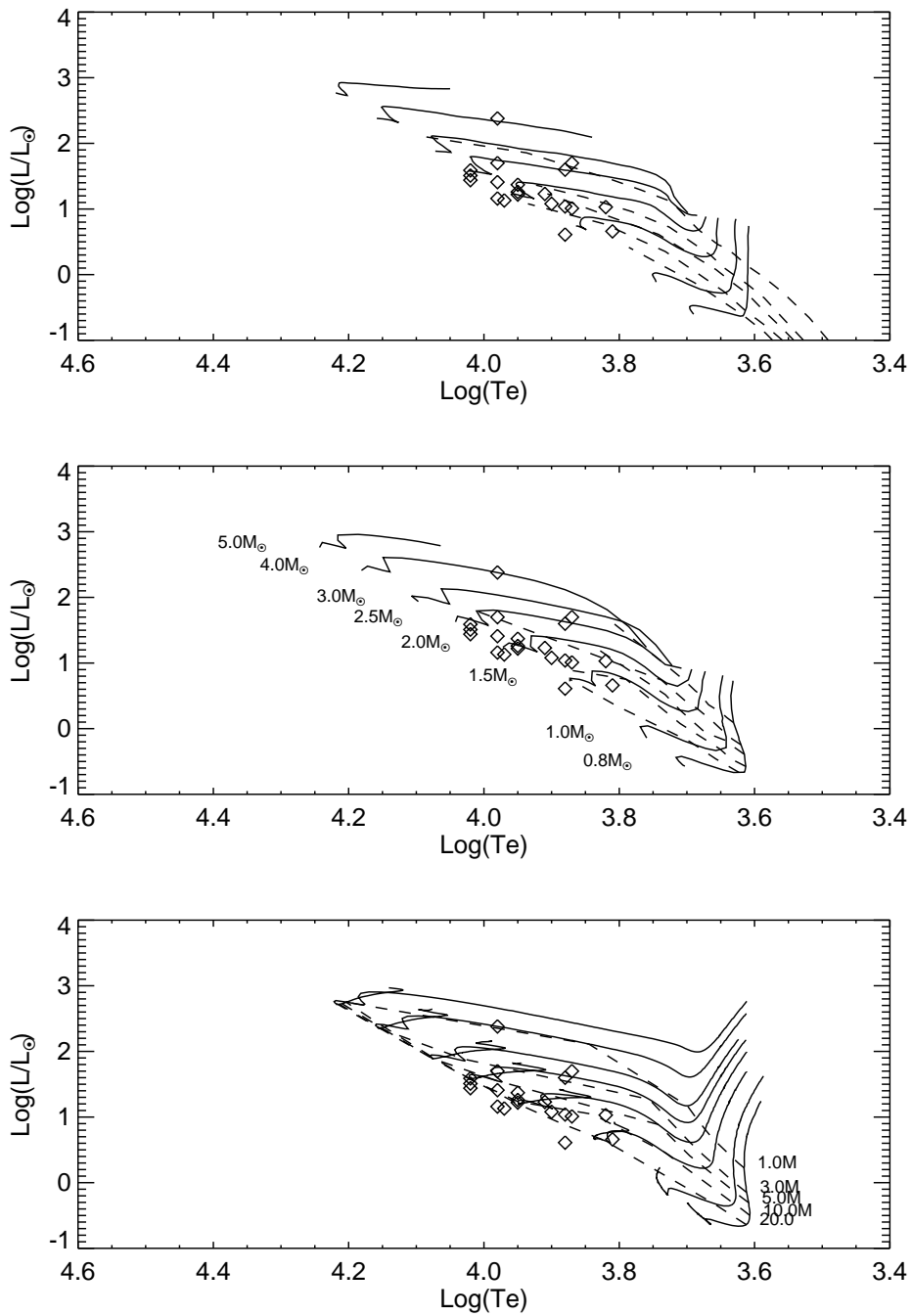


Figure 4.1 Evolutionary Tracks with Stars. We plotted our program stars over figure 2 and obtained the above figure. We interpolated to find precise values from this figure. The result is shown in 1.

Additionally, they argue that HAeBe stars typically have an accretion rate of  $\leq 10^{-7} M_{\odot} yr^{-1}$ . According to Palla & Stahler (1992), the effect on the birthline due to higher accretion rate is a shift towards the top right on a HR diagram. Since our stars have a lot lower accretion rate than the one they used, a model with lower accretion rate would possibly incorporate our stars which fall below the ZAMS. We also noticed that Bernasconi (1996) claims to have used a time-dependent accretion rate, however, their model did not seem to be that different from Palla & Stahler (1993). We differ this discussion to a later paper.



# Chapter 5

## Conclusion

While trying to find the ages and masses for our 20 Herbig Ae/Be stars, we realized that the values we calculated were not consistent with what we found in the literature. Our results are shown in table 1. We then decide to compare the age and mass using 3 different well-cited models – Palla & Stahler(1993), Bernasconi (1996) and Siess et al(2000). These models are described in section 2. We found that the masses we calculated were consistent, however, the ages varied by a factor of 2 to 3. This, we quickly realized, is due to the effect of different physical characteristics of the models as discussed in section 2. Finally we address the stars that fall below the ZAMS on the HR diagram, in section 4. We defer the discussion on this topic to a later paper.

As a consequence of this discrepancy, a problem one would encounter is in deciding which model estimates the ages of the star most accurately. We realized are relative to the initial state of the star or the birthline. This means that we can expect the ages determined from these models to differ from each other. We thus conclude that if an astronomer is attempting to determine an intrinsic property of a star, then one should carefully choose a model that is closest fit to the star to determine these parameters. However, if the astronomer is comparing ages or other properties inferred from age

of different stars then it would be more relevant to make sure that the ages were computed using the same model. Otherwise, the conclusions drawn from these ages might be skewed or inaccurate.

# Bibliography

- [1] Palla, & Stahler 1990, ApJ, 357, 288
- [2] Siess et al. 2000, ApJ, num, num
- [3] Bernasconi, P. A. 1996, ApJ, 120 , 57
- [4] Acke, B. & van den Ancker, M. E. 1998, A&A, 357, 325
- [5] Malfait, K., Bogaert, E, & Waelkens, C. 1998, A&A, 331, 211
- [6] Herbig, G. H. 1960, ApJ, 4,337H
- [7] Hernández, Jesús et al. 2004, ApJ, 127, 1682H
- [8] Palla, & Stahler 1994, ASPC, 64, 391P
- [9] Palla, & Stahler 1993, ASPC, 40, 437P

